

Soft Haptic Display Toolkit: A Low-Cost, Open-Source Approach to High Resolution Tactile Feedback

Pijuan Yu, Alexis Urquhart, Anzu Kawazoe, Thomas K. Ferris, M. Cynthia Hipwell, Rebecca F. Friesen

Abstract—High-spatial-resolution wearable tactile arrays have drawn interest from both industry and research, thanks to their capacity for delivering detailed tactile sensations. However, investigations of human tactile perception with high-resolution tactile displays remain limited, primarily due to the high costs of multi-channel control systems and the complex fabrication required for fingertip-sized actuators. In this work, we introduce the Soft Haptic Display (SHD) toolkit, designed to enable students and researchers from diverse technical backgrounds to explore high-density tactile feedback in extended reality (XR), robotic teleoperation, braille displays, navigation aid, MR-compatible somatosensory stimulation, and remote palpation. The toolkit provides a rapid prototyping approach and real-time wireless control for a low-cost, 4×4 soft wearable fingertip tactile display with a spatial resolution of 4 mm. We characterized the display’s performance with a maximum vertical displacement of 1.8 mm, a rise time of 0.25 second, and a maximum refresh rate of 8 Hz. All materials and code are open-sourced to foster broader human tactile perception research of high-resolution haptic displays.

I. INTRODUCTION

The concept of the “metaverse,” first proposed in 1992, has recently regained popularity and has led to the development of various creative wearable haptic actuators and devices for actively interacting with virtual environments [1], including vibrotactile feedback for virtual textures [2] and multiple degrees of freedom (DOFs) force feedback driven by parallel rigid kinematics [3]. Among these different techniques, soft haptic actuators present advantages and potential for wearable haptics because of their high spatial resolution, wearability, and safety [4], [5], [6].

Many high-resolution soft fingertip displays are driven by electroosmotic [7], electrohydraulic [8], chemical reaction-based [9], or micro-pump actuation methods [10], [11], [12]. Among these, pneumatic actuators—which generate tactile sensations through fluid pressure—are particularly popular in both the haptics and soft robotics communities due to their relative ease of fabrication, scalability, and controllability. While several soft robotics toolkits have been developed to simplify pneumatic control systems [13], [14], [15], research on high-resolution pneumatic fingertip displays remains limited, primarily due to high costs or complex actuator fabrication processes [5], [10], [11].

For instance, the commercial HaptX G1 glove integrates up to 135 microfluidic actuators across the fingers and palm

This work was supported in part by the National Science Foundation Grant 2326453. Pijuan Yu, Alexis Urquhart, Anzu Kawazoe, M. Cynthia Hipwell, and Rebecca F. Friesen are with Mechanical Engineering, Texas A&M University, College Station, Texas. Email: pijuanyu@tamu.edu

Thomas K. Ferris is with Department of Industrial & Systems Engineering, Texas A&M University, College Station, Texas.

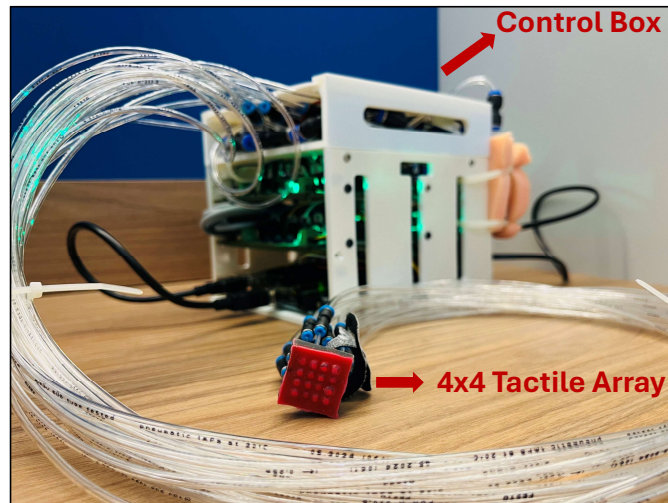


Fig. 1. Overview of Soft Haptic Display (SHD) System. The 4 × 4 tactile array haptic display (22 x 22 x 7 mm, red) is connected to the control box (white) via transparent air tubes (one meter). The control box communicates with the laptop wirelessly using a socket communication method.

[12], but its Mobile Airpack Edition is priced at \$38,990 [16], making it inaccessible to many researchers. While recent studies propose lower-cost alternatives, they often impose stringent fabrication requirements, such as laser cutting [7], [8] or plasma bonding [8], [10], creating a significant barrier to entry for students and researchers interested in high-resolution tactile feedback.

To address these limitations, we introduce the Soft Haptic Display (SHD) toolkit. Building on principles from existing soft robotics toolkits, the SHD is accessible to students and researchers with diverse technical backgrounds, enabling them to create custom high-resolution tactile arrays worn on the fingertip to provide high-density force feedback. The contributions of this work are summarized as follows:

- Design details of a fingertip-sized 4 × 4 soft wearable tactile array.
- A desktop-sized, lightweight (1.832 Kg) control box that provides real-time control of the tactile array.
- Proportional pressure regulation, 16 binary pressure outputs, and 8 pressure sensor inputs.
- 0.25 seconds actuator rise time, achieving 1.80 mm maximum vertical displacement with up to 8 Hz refresh frequency.
- A user-friendly graphical interface for wireless, independent control of the tactile display with low latency.

In addition to creating immersive interactions in virtual environments [1], this system supports robotic teleoperation

[17], refreshable Braille displays [18], [19], brain-activity mapping via somatosensory stimulation in MRI settings [20], spatial orientation and navigation [21], remote palpation [22], and various psychophysical studies. Our goal is to advance high-resolution haptic display research by offering a low-cost, rapidly developed wearable tactile array, and we have open-sourced all project resources at the repository below¹.

The remainder of this paper is structured as follows. First, we describe the state of the art in open-source soft actuator systems, as well as high-resolution tactile array research. Then, we outline the fabrication process for the custom tactile array. Next, we detail the control platform, including hardware components, the low-level controller, and the user interface. Finally, we present the device characterization results—displacement, pressure, response time, and refresh frequency—to evaluate the system’s performance.

II. RELATED WORK

A. Open Source Soft Robotics Systems

Soft robotics is a rapidly growing field of research due to its adaptability, flexibility, and safety for human-robot interaction and haptics applications. A popular resource for new researchers and students to learn soft robotic design is the Soft Robotics Toolkit (SRT) [13]. As an open-access website, it provides detailed documentation of the design process for soft pneumatic actuators and a pneumatic control board for low-level control. Another option is the FlowIO miniature modular platform, which aims to guide students and researchers in actuating and sensing soft wearable robots through its five pneumatic ports and various modular components [14]. Other open-source websites related to soft robotics include Programmable Air [23], PneuSoRD [24], Pneumatic Controller [25], and Pneuduino [26]. These pneumatic systems aim to achieve pressure regulation through closed-loop feedback control using pressure sensors and valves. However, when actuating 2 mm bubbles in a fingertip-sized wearable tactile array, controlling airflow by frequently switching binary valves with a Pulse Width Modulation (PWM) signal causes vibrations due to pressure fluctuations [27]. While replacing binary valves with proportional solenoid valves may reduce vibration, the size and cost of proportional valves are significantly higher, making them less suitable for high-resolution tactile arrays.

Instead of developing a custom regulator, an alternative approach is to directly control a commercial analog pressure regulator. For instance, the Soft Robotics Control-Unit [15] is an open-source platform that uses piezo pressure regulators to teleoperate a soft gripper, actuate a soft Pneumatic Unit Cell (PUC) for vibrotactile and force feedback in virtual reality (VR) [28], and control a large area haptic display with four groups of PUCs [29]. Similarly, Meta Reality Lab proposed a multichannel pneumatic system with approximately 15 identical pressure regulators to control a pneumatic wristband [30]. While the size and performance of these commercial pressure regulators are significantly better than

custom pressure regulators, they cost around \$700 each, which is unaffordable for high-resolution tactile displays.

B. Fabrication Methods of Advanced Tactile Array

Rigid actuator technologies—such as shape-memory-alloy (SMA) springs [19], [31] and motorized sliders [32], [33]—are popular for high-resolution tactile arrays because they are inexpensive and easy to manufacture. However, their intrinsic rigidity limits conformability, slows response times, and lacks the biomimetic softness required for wearable haptics and safe human–robot interaction.

Soft pneumatic and hydraulic actuators address these shortcomings by emulating biological tissue mechanics, but they typically require sophisticated fabrication tools. For example, Wu et al. presented a 2×3 pneumatic array, which utilized a UV lithography machine for mold creation and a Parylene deposition system for coating [34]. Shen et al. developed a 32-bubble fingertip actuator driven by the electroosmotic method, with components precisely cut using an ultraviolet laser cutter (LPKF U4) and a CO2 laser cutter (ULS VLS 4.60) [7]. Meta Reality Lab introduced a high-resolution electrohydraulic haptic interface comprising 16 individually controlled bubble actuators [8]. Their fabrication process involved laser cutting a thermoplastic dielectric film with 8 holes and using a plasma bonding machine to bond a thin silicone sheet to one side of the dielectric film. Shan et al. developed a microfluidic 5×5 tactile array, employing a vacuum oven to degas and cure PDMS (RTV615) solution and a plasma cleaner to enhance bonding between layers [10]. Wang et al. [11] demonstrated a 4×4 pneumatic array fabricated by bonding two layers of thermoplastic polyurethane (TPU) films using a hot press machine and custom aluminum alloy stamps.

While the aforementioned studies leveraged advanced manufacturing methods to fabricate tactile arrays and achieve higher performance, the reliance on expensive and complex fabrication tools poses significant barriers for students and researchers from diverse backgrounds who aim to rapidly develop high-resolution tactile arrays.

III. MATERIAL AND METHODS

The SHD system architecture is illustrated in Fig. 2 and includes three data flows: control signals (green), power supply (red), and airflow (blue). Overall, the air pressure is generated by the micro pump, regulated by the pressure regulator, distributed into 16 channels via mini solenoid valves, and then directed to the silicone tactile array to inflate the bubbles. The host PC communicates with the Raspberry Pi and Arduino Uno to adjust the system pressure and control the valves for the high-resolution display. Details are described in the following subsections.

A. Tactile Array Design

The 4×4 tactile array consists of 16 hollow, bottomless cylindrical channels arranged within a 22 mm square grid. It is composed of two layers (Fig. 3): 4 mm of Dragon Skin 10 Medium and 3 mm of EcoFlex 00-10. Dragon Skin was

¹github.com/pijuanyu2022/Soft-Haptic-Display-Toolkit

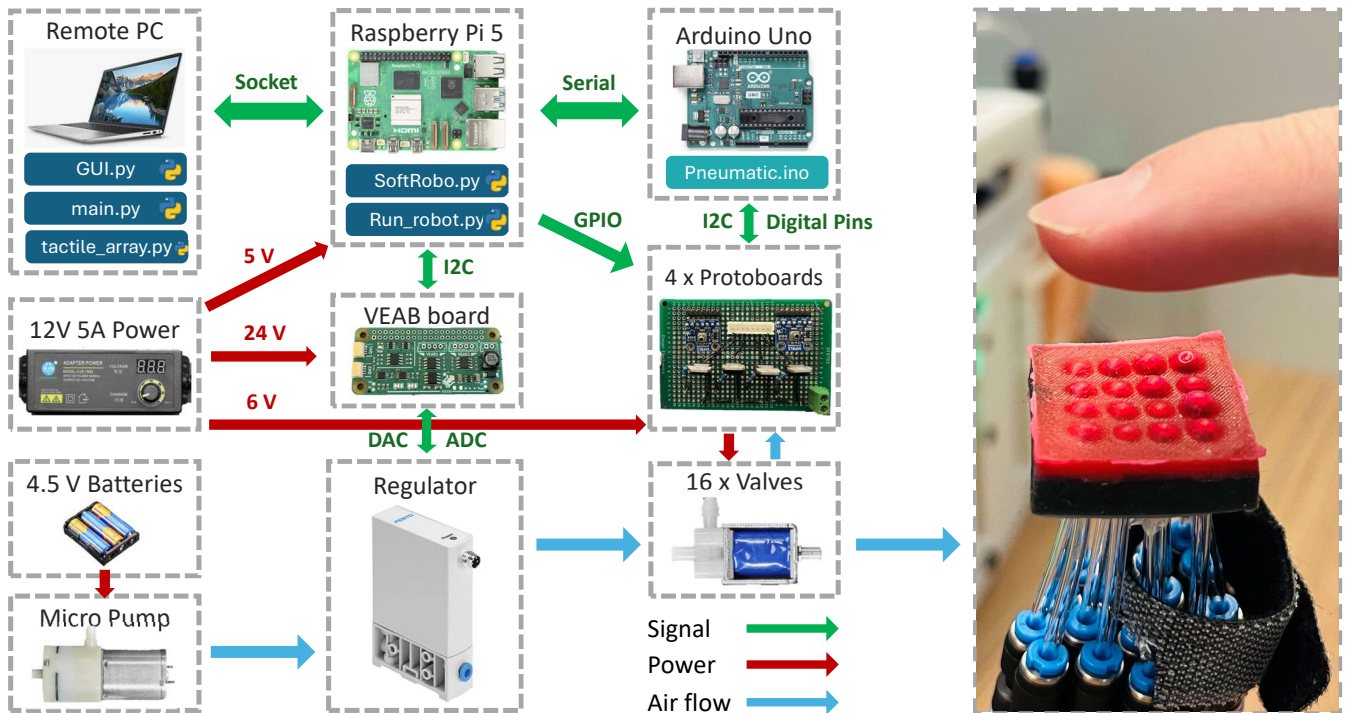


Fig. 2. **System architecture.** The entire system, except for the host PC, is housed within the control box. Users can operate the graphical user interface (GUI) on the host PC to wirelessly control one pressure regulator and 16 solenoid valves for pattern display on the 4×4 tactile array.

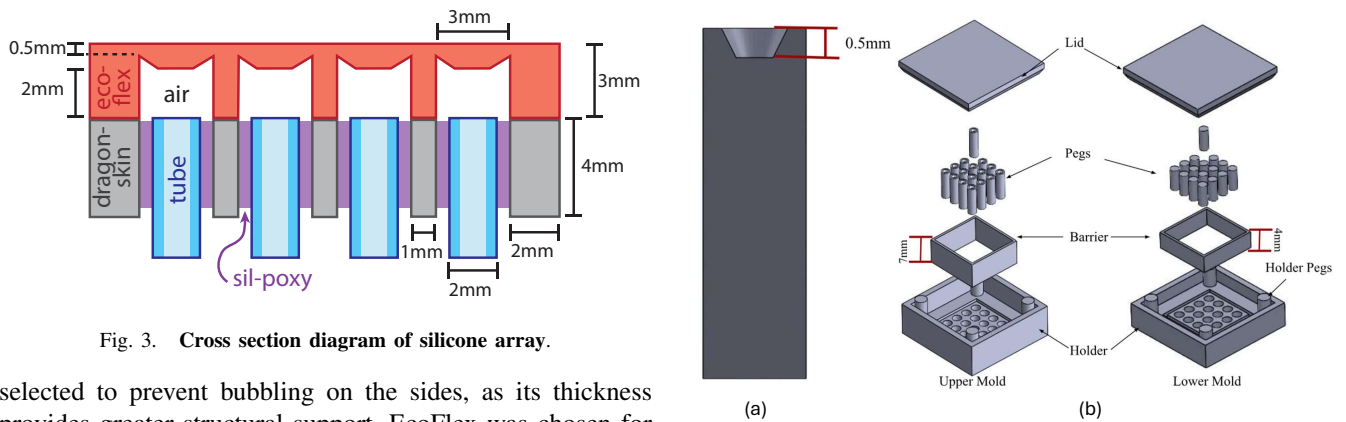


Fig. 3. **Cross section diagram of silicone array.**

selected to prevent bubbling on the sides, as its thickness provides greater structural support. EcoFlex was chosen for its low tensile strength and high elasticity, allowing for temporary deformation at the top. To reinforce the center, which experiences the highest stress, the tops gradually increase in thickness from 0.5 mm at the edges to 1 mm in the middle, resulting in a 0.5 mm difference in thickness.

The arrays were molded in two parts (Fig. 4A): the lower layer and the upper layer. The molds were produced using Prusa's MK3S+ FDM (Fused Deposition Modeling) printers with PLA (Polylactic Acid). They were designed to be modular to prevent tearing during demolding (see Fig. 4B). Before molding, the molds were prepped with silicone release spray. The lower layer was molded first: Dragon Skin 10 Medium was hand-mixed for three minutes to ensure thorough blending. It was then degassed in a vacuum chamber at -68 kPa (gauge) for five minutes. Once bubbling ceased, the solution was removed from the vacuum chamber and slowly and evenly poured into the mold. The mold was then placed back into the vacuum chamber at 20

inHg for three minutes to remove any remaining air bubbles. The lids, connected to the holder through pegs, were placed on top to create an even surface. The molds were left to cure at room temperature for five hours.

Once cured, the lower layer was removed from the mold and placed at the bottom of the upper mold. The EcoFlex 00-10 was prepared using the same steps as the Dragon Skin 10 Medium and was poured directly on top of the lower layer. This layer was left to cure for four hours. Once the final array was removed from the mold, 2 mm OD (outer diameter) plastic tubing, cut to 35 mm in length, was added. SilPoxy was applied in a thick layer to the bottom of each plastic tube, ensuring none covered the tubing hole. Each tube was then inserted fully into its respective hole and subsequently pulled up by 2 mm from the bottom of the tactile array. The

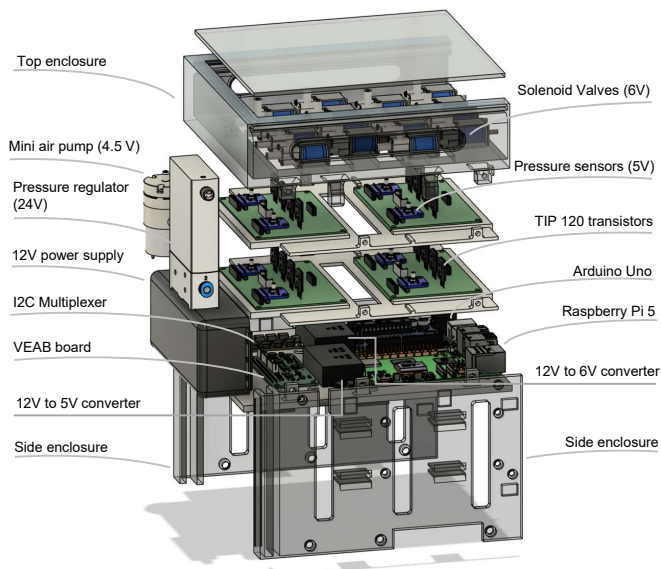


Fig. 5. **SHD Controller Box Details.** The control box measures 20 cm in length, 15 cm in width and 15 cm in height. All enclosure components and board holders are 3D-printed using PLA material.

SilPoxy was allowed to cure for 30 minutes before use.

B. Hardware system

The SHD hardware system is organized into three functional layers within a controller box, with an additional rear module dedicated to power and air supply (see Fig. 5). The bottom layer houses a Raspberry Pi 5 (8 GB RAM) mini-computer, an Arduino Uno Rev3 micro-controller, an I2C multiplexer (PCA9548A, Adafruit), a VEAB board, and two DC voltage converters. The Raspberry Pi 5 serves as the central controller, enabling wireless communication with a host PC, serial communication with the Arduino Uno, and direct control of the pressure regulator via the VEAB board. The Arduino Uno is connected to the I2C multiplexer to support up to eight I2C channels.

The VEAB board is connected to a proportional piezo regulator (VEAB-L-26-D13-Q4-V1-1R1, Festo) capable of providing 0–0.1 MPa of output pressure in response to a 0–10 V input. An mini air pump (4699, Adafruit) supplies air at a maximum pressure of 55 kPa and a flow rate of up to 2.5 liters per minute. The VEAB board incorporates two digital-to-analog converters (MCP4725, MicroChip) to deliver control signals and two analog-to-digital converters (ADS1014, Texas Instruments) to receive feedback from the regulator. Further details of the VEAB board can be found in the Soft Robotics Control-Unit [15].

The middle layer of the controller box contains four custom circuit boards. Each board integrates four TIP120 transistors (976, Adafruit) for switching solenoid valves on or off, four 1N4001 flyback diodes (755, Adafruit) to prevent reverse voltage damage, and two MPRLS pressure sensors (3965, Adafruit) rated for 0–172 kPa. Twelve of the transistors interface with the Arduino’s digital outputs, while the remaining four interface with the Raspberry Pi’s GPIO digital outputs. All eight pressure sensors communicate with

the Arduino via the I2C multiplexer for data acquisition.

The top layer includes 16 solenoid micro air valves (6V Air Valve, Adafruit). A 12 V adjustable power supply (4880, Adafruit) mounted at the rear of the controller box provides the primary power input. This supply is routed through the VEAB board to generate 24 V for the pressure regulator (after voltage amplification), through a DC converter (12 V to 5 V USB Type-C, YIPIN HEXHA) for powering the Raspberry Pi, and through another DC converter (12 V to 6 V Step Down Converter, DROK) for driving the 16 solenoid valves (see Fig. 2). The Arduino Uno receives power from the Raspberry Pi, which also indirectly supplies the eight pressure sensors through the I2C multiplexer. Due to the high current demand of the micro air pump, a separate 4.5 V battery box is used to power it.

C. Software architecture

The control signal flow is represented as the green line in Fig. 2. To achieve wireless control, the host PC first utilizes the Secure Shell Protocol (SSH) to remotely log into the Raspberry Pi and launch the Python script. The host PC then launches Python software with a graphic interface in the local environment and establishes a connection to the Raspberry Pi via socket communication using the Transmission Control Protocol/Internet Protocol (TCP/IP) network. The Raspberry Pi and Arduino Uno communicate through a USB cable using a serial communication method. This setup offers several benefits: the TCP/IP network enables low-latency communication (typically 1–10 ms) and high data transfer rates, ensuring reliable and real-time interaction. Additionally, the USB-serial connection allows a communication frequency of up to 115200 bps, supporting efficient data exchange between the Raspberry Pi and Arduino.

To offer users—including students, researchers, and practitioners—the flexibility to control a high-resolution tactile array, debug the system, visualize pressure sensor data, and preserve records for future analysis, a user-friendly graphical user interface (GUI) was developed using the CustomTkinter Python library. The GUI is organized into four primary panels, each serving a distinct purpose in the configuration and operation of the tactile system (Figure 6). The sections below provide detailed descriptions of these panels.

1) *Setting Panel:* The first panel (Figure 6A), referred to as the Setting Panel, is central to managing the system’s core configurations. Through a concise set of controls, users can establish a direct connection to the Raspberry Pi by entering its IP address in a pop-up window, restore the system to default settings, and archive both actuator commands and pressure sensor data into CSV files that include time stamps for traceability. Additionally, the interface appearance can be toggled between Light and Dark modes, and its scale can be adjusted from 80% to 120%, accommodating various monitor sizes and user preferences.

2) *Pressure Regulator Panel:* The Pressure Regulator Panel (Figure 6B) comprises three integrated sections designed to fine-tune the system’s internal pressure. On the left, a real-time plot visualizes the normalized control signal

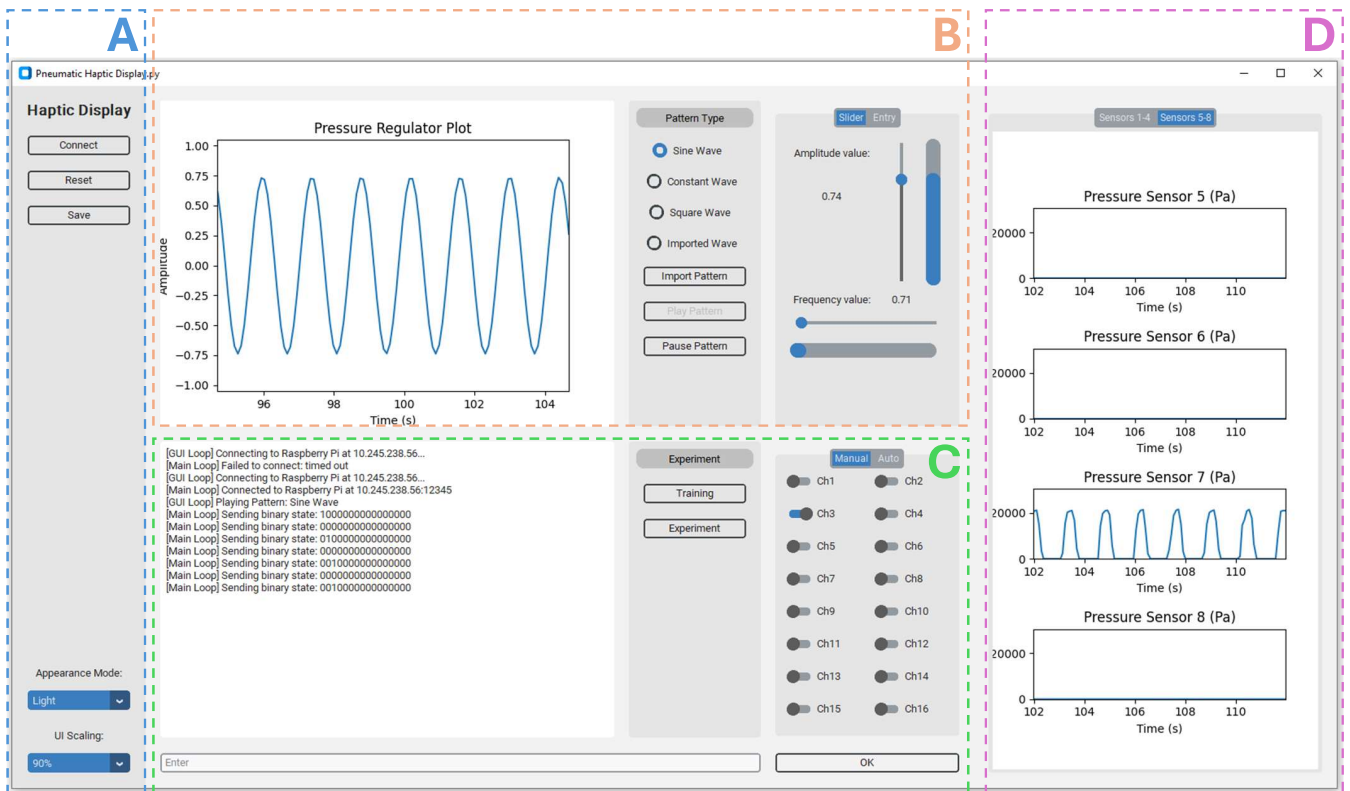


Fig. 6. **Graphical User Interface (GUI).** (A) Setting panel; (B) Pressure regulator panel; (C) Display panel; (D) Sensor panel.

over time, enabling users to observe how the voltage applied to the regulator is dynamically adjusted. In the middle section, several waveforms—sinusoidal, square, constant, and custom-imported waveforms—can be selected to control the pressure inside the system. Of these, the constant waveform is often used to maintain a uniform pressure for stable force output across the array. The right section allows users to modify parameters such as amplitude for sinusoidal, square, and constant waveforms, while frequency can be tuned for sinusoidal and square waves. Both slider-based and direct text-entry methods are supported, ensuring precision and flexibility in the parameter settings.

3) *Display Panel*: The Display Panel (Figure 6C) facilitates real-time feedback and provides direct valve control for the tactile array. A log window on the left chronicles all user inputs and system messages, streamlining troubleshooting efforts. The middle portion of this panel manages the launching of additional windows for psychophysical or other specialized experiments. On the right, 16 interactive toggle buttons correspond to the array’s 16 valves, enabling users to manually activate or deactivate individual channels to create custom patterns. An Auto tab offers an assortment of pre-programmed animation sequences for demonstration purposes and device testing. Moreover, researchers can design and add their own animation patterns through this tab. In order to support ease of use, a “help” command can be entered into a dedicated text box at the bottom of the panel, and a concise tutorial will then be displayed within the log window.

4) *Sensor Panel*: The final panel (Figure 6D), called the Sensor Panel, contains eight real-time plots illustrating the

pressure sensor data over time. To facilitate monitoring, these plots are grouped into two tabbed views, covering sensors 1–4 and sensors 5–8, respectively. By providing immediate visual feedback on the sensor readings, the panel assists users in diagnosing potential airflow or pressure inconsistencies within the system. Furthermore, the panel’s modular design can easily be extended to incorporate additional sensors, ensuring that the GUI will scale as the hardware evolves.

IV. DEVICE CHARACTERIZATION

To understand the characteristics of the haptic device, we conducted measurement experiments.

A. Dynamic response and delay in single bubble actuation

First, we measured the displacement of a single bubble using a Laser Doppler Vibrometer (VibroFlex QTec, Polytec, USA). Simultaneously, the input signal to the pressure regulator and the pressure from the internally mounted pressure sensor were recorded. The Laser Doppler Vibrometer (LDV) and the input signal to the pressure regulator were captured using a data acquisition (DAQ) device (NI USB-6211, National Instruments, USA) at a sampling rate of 1000 Hz. The velocity data obtained from the LDV was converted to displacement through numerical integration. The pressure sensor readings were recorded by an Arduino at a sampling rate of 10 Hz. Using the input signal as a reference, we plotted the input signal to the pressure regulator, the displacement, and the pressure of a single bubble for sine and square wave inputs at frequencies of 0.5, 1, and 2 Hz (Fig. 7A).

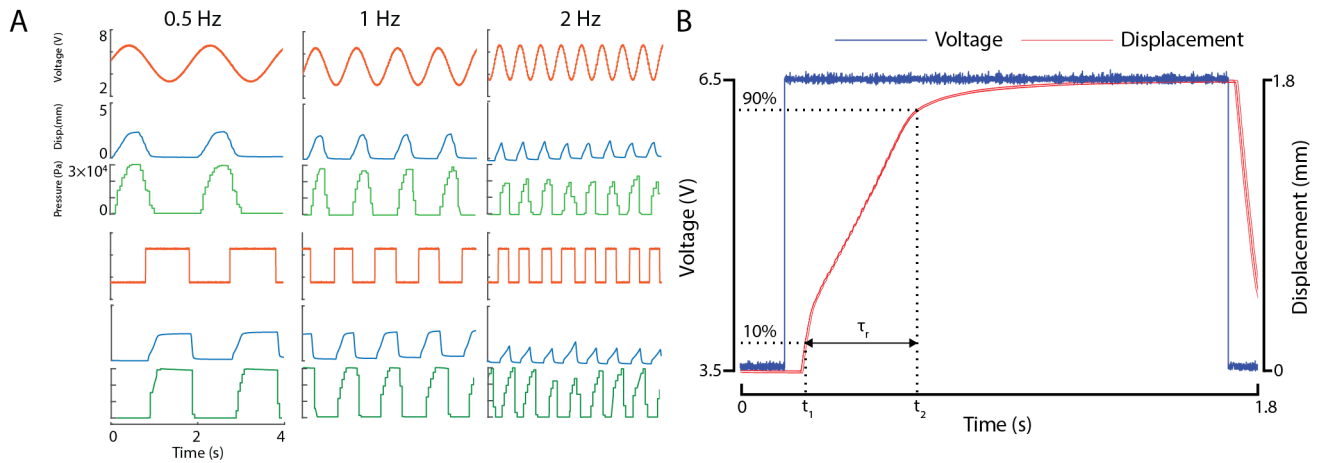


Fig. 7. **Input Signal and Displacement of a Single Bubble** (A) Time course of the input signal to the pressure regulator (orange, voltage in V), bubble displacement (blue, mm), and resulting pressure (green, Pa). (B) Single-bubble displacement response to a 0.5 Hz square wave input. Rise time ($\tau_r = t_2 - t_1$), defined as the interval between 10% (t_1) and 90% (t_2) of maximum displacement, is 0.25 s under safe operation (6.5 V input, 30 kPa pressure, 1.8 mm displacement).

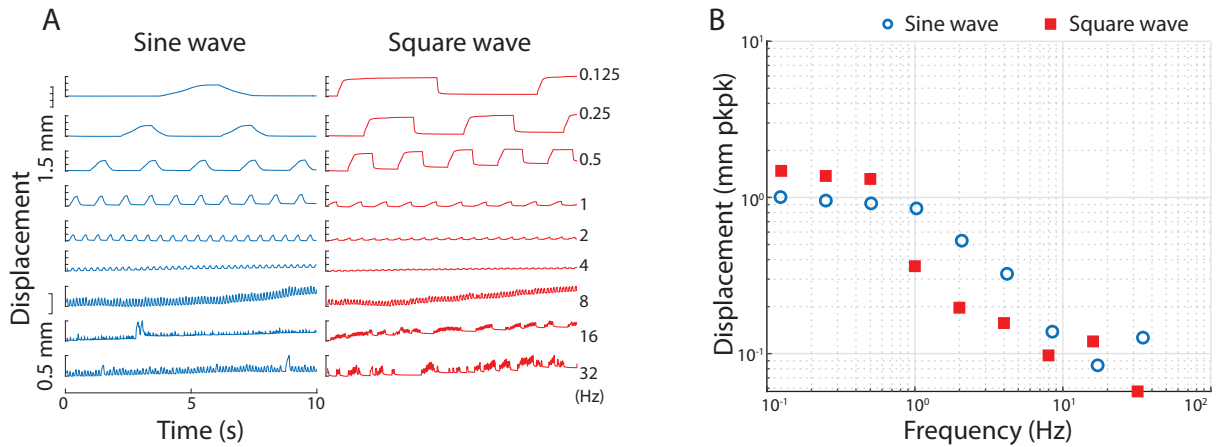


Fig. 8. **Relationship Between Input Frequency and Displacement of a Single Bubble** (A) Displacement of a single bubble at 9 different input frequencies of sine and square waves. (B) Relationship between input frequency and bubble displacement for both sine and square wave inputs. The light dashed line represents the curve-fitting model for the sine wave, while the pink dashed line represents the curve-fitting model for the square wave.

Next, we calculated the delay between the input signal to the pressure regulator and the corresponding bubble displacement. Figure 7B shows the alignment of one cycle of the 0.5 Hz square wave input and its resulting displacement. During the measurements, we recorded five cycles of the square wave over a 10-second period, and the displacements for all five cycles were plotted. As shown in Fig. 7B, the displacement of the bubble across the five cycles was consistent. To determine the delay, we measured the time lag between the rising edges of the input voltage signal and the corresponding displacement. The calculated rising time was 0.25 seconds, and this value remained consistent across all cycles of the square wave input.

Latency in the system was measured by recording timestamps from both the GUI and the Raspberry Pi for corresponding events, specifically when the user clicked a button and when the sensor data exceeded 1 kPa. Synchronized via the Network Time Protocol (NTP), the time difference between user inputs and sensor events was 164.65 ± 37.42 ms latency across 15 trials.

B. Frequency Characterization

In the second part of the measurement, we investigated the extent to which a single bubble actuates when subjected to different input frequencies of sine and square waves. To achieve this, we measured the displacement of the bubble using a laser Doppler vibrometer (LDV). The input signals included sine and square waves at frequencies of 0.125, 0.25, 0.5, 1, 2, 4, 8, 16, and 32 Hz. Figure 8A illustrates the displacement of a single bubble when exposed to the nine different frequencies of sine and square waves. As expected, maximum displacement decreased progressively between 0.5 Hz and 8 Hz as frequency increased. However, irregular response was observed at 16 Hz and 32 Hz, likely attributable to wireless communication latency and pressure fluctuations induced by the 1-meter pneumatic tubing.

We calculated the peak-to-peak displacement, defined as the difference between the initial state and the maximum displacement for each frequency, and plotted the relationship between input frequency and bubble displacement (Figure 8B). As shown in Figure 8B, the displacement varies

TABLE I
EXISTING MICROFLUID FINGERTIP WEARABLE HIGH RESOLUTION HAPTIC DISPLAY

Tactile Device	Actuation Method	Array size	Actuator Fabrication Method	Vertical Displacement (mm)	Spatial Resolution (mm)	Diameter (mm)
2012 [34]	Pneumatic	2 x 3	UV lithography, Parylene coating	0.56	2.50	1.40
2023 [12]	Pneumatic	16	Proprietary microfluidic system (HaptX)	0.90	2.50	Unknown
2023 [7]	Electroosmosis	32	Ultraviolet laser cutting, CO ₂ laser cutting	1.10	2.36	1.60
2023 [8]	Electrohydraulic	4 x 4	Laser cutting, Plasma bonding	2.00	3.00	1.50
2024 [11]	Pneumatic	4 x 4	Hot press, Custom stamps	2.50	4.00	2.50
2024 [10]	Pneumatic	5 x 5	Vacuum oven, Plasma bonding	0.21	1.25	0.75
Our work	Pneumatic	4 x 4	3D printer, Vacuum chamber	1.80	4.00	3.00

across different frequencies and wave types. However, a general trend is observed where the displacement decreases as the input frequency increases.

V. DISCUSSION AND FUTURE WORK

A. Contributions

In this study, we present the development of the Soft Haptic Display (SHD) toolkit, which includes the fabrication of a soft fluidic tactile array, firmware integration, and user interface (UI) design. The primary goal of the SHD is to provide a rapid prototyping platform that lowers the barriers to entry for researchers in wearable, high-resolution tactile feedback. The total cost of this toolkit is approximately \$1,000, including a \$700 pressure regulator, which remains significantly more affordable than the HaptX glove and other high-density arrays with comparable spatial resolution. Although less-expensive devices exist (e.g., the stepper-driven TactionTablet at \$32 [33] or jamming-based displays at \$400 [35]), the SHD combines fingertip-sized actuators and soft compliance—features that are essential for applications such as VR tactile feedback and telerobotic manipulation.

To facilitate ease of prototyping, our novel soft actuator and control box require only a 3D printer and a vacuum chamber for fabrication, utilizing widely available materials such as silicone rubber and PLA filament. For wireless control with low latency, the system integrates a Raspberry Pi 5 and an Arduino Uno. Both platforms benefit from large user communities that provide tutorials, troubleshooting resources, and support for a wide range of peripherals, accelerating development and reducing the learning curve. Additionally, the toolkit features a modern, customizable UI built with an open-source Python library, allowing users to control the tactile display in real time and monitor dynamic pressure values. The project repository includes comprehensive documentation, covering component procurement, tactile array fabrication, control board soldering, system assembly, and software installation and execution.

In terms of performance evaluation, our device characterization results indicate performance comparable to other high-resolution soft tactile devices (see Table I). The spatial resolution—defined as the center-to-center distance between adjacent actuator chambers—is 4 mm, with each chamber having a 3 mm diameter, resulting in an edge-to-edge separation of only 1 mm. In order to avoid popping the array bubbles, we limit maximum control voltage input to the regulator below 6.5 V, corresponding to a maximum 30 kPa

of pressure and 1.8 mm step response displacement with a rise time of 0.25 seconds. Furthermore, the microvalves and pump are housed within a compact 20 × 15 × 15 cm control box, reducing reliance on bulky air supply systems and enabling a portable, backpack-compatible design.

B. Limitations and Future work

Despite these advancements, several limitations merit attention. First, while the SHD’s cost is substantially lower than commercial systems, the \$700 pneumatic regulator remains prohibitive for independent developers or resource-constrained settings. Future efforts will prioritize open-source regulator designs or alternative pressure sources to further democratize access.

Second, the pressure control system currently limits individual actuator modulation. While each actuator unit can be independently toggled on or off through the valve, individual height control is difficult to achieve due to the system’s open-loop design. Instead, all 16 actuators are modulated simultaneously by a single pressure regulator. The primary reason is that we utilized low-cost ON/OFF solenoid valves to minimize costs, which limits precision.

Although we attempted to develop a bang-bang closed-loop control using two valves and a pressure sensor, following the approach in [36], applying this method in a low-pressure (30 kPa) pneumatic system led to air fluctuations and vibrations that propagate through the tubing and become perceptible to the user. Future research should explore advanced pneumatic control techniques and conduct a force characterization experiment to evaluate performance.

The third limitation is the lack of psychophysical experiments. While we characterized the device’s performance using the LDV and pressure sensor, human perception studies are essential. Specifically, we plan to conduct an absolute threshold detection experiment to determine the minimum perceivable pressure for tactile stimulation and a pattern discrimination experiment to evaluate the device’s ability by rendering both static and dynamic tactile patterns.

The final limitation is that, while the toolkit provides a custom GUI, it currently lacks demonstrations for AR/VR applications. Additionally, the control box is still powered by a grounded power supply, which restricts untethered operation. Future work will focus on replacing the grounded power supply with a battery, enabling the control box to function as a wearable backpack. Furthermore, efforts will be directed toward integrating the tactile display with Unity to facilitate AR/VR-based interactions.

VI. CONCLUSION

In this paper, we introduced the Soft Haptic Display (SHD) toolkit, which offers a rapid prototyping approach for developing soft microfluidic tactile arrays capable of high-resolution force feedback. By simplifying design, fabrication, and operation, the toolkit aims to lower barriers for students and researchers in haptics, soft robotics, extended reality, assistive technology, neuroscience, psychophysics, and other fields exploring high-density microactuator-based tactile feedback. The toolkit includes detailed instructions on installation, assembly, and usage, and all resources are available open-source. We invite interested researchers to make use of this toolkit, thereby expanding the horizons of human tactile perception research and advancing the development of high-resolution haptic displays.

ACKNOWLEDGMENT

This work was supported by the US National Science Foundation (NSF-2326453).

REFERENCES

- [1] C. Pacchierotti, F. Chinello, K. Koumaditis, M. D. Luca, E. Ofek, and O. Georgiou, "Guest editorial haptics in the metaverse: Haptic feedback for virtual, augmented, mixed, and extended realities," *IEEE Transactions on Haptics*, vol. 17, no. 2, pp. 122–128, 2024.
- [2] R. F. Friesen and Y. Vardar, "Perceived realism of virtual textures rendered by a vibrotactile wearable ring display," *IEEE Transactions on Haptics*, vol. 17, no. 2, pp. 216–226, 2024.
- [3] S. B. Schorr and A. M. Okamura, "Fingertip tactile devices for virtual object manipulation and exploration," in *Proceedings of the 2017 CHI conference on human factors in computing systems*, 2017, pp. 3115–3119.
- [4] A. Frisoli and D. Leonardis, "Wearable haptics for virtual reality and beyond," *Nature Reviews Electrical Engineering*, pp. 1–14, 2024.
- [5] M. Emami, A. Bayat, R. Tafazolli, and A. Qudus, "A survey on haptics: Communication, sensing and feedback," *IEEE Communications Surveys & Tutorials*, 2024.
- [6] M. Zhu, S. Biswas, S. I. Dinulescu, N. Kastor, E. W. Hawkes, and Y. Visell, "Soft, wearable robotics and haptics: Technologies, trends, and emerging applications," *Proceedings of the IEEE*, vol. 110, no. 2, pp. 246–272, 2022.
- [7] V. Shen, T. Rae-Grant, J. Mullenbach, C. Harrison, and C. Shultz, "Fluid reality: High-resolution, untethered haptic gloves using electroosmotic pump arrays," in *Proceedings of the 36th Annual ACM Symposium on User Interface Software and Technology*, 2023, pp. 1–20.
- [8] J. Hartcher-O'Brien, V. Mehta, N. Colonnese, A. Gupta, C. J. Bruns, P. Agarwal *et al.*, "Fingertip wearable high-resolution electrohydraulic interface for multimodal haptics," in *2023 IEEE World Haptics Conference (WHC)*. IEEE, 2023, pp. 299–305.
- [9] R. H. Heisser, C. A. Aubin, O. Peretz, N. Kincaid, H. S. An, E. M. Fisher, S. Sobhani, P. Pepiot, A. D. Gat, and R. F. Shepherd, "Valveless microliter combustion for densely packed arrays of powerful soft actuators," *Proceedings of the National Academy of Sciences*, vol. 118, no. 39, p. e2106553118, 2021.
- [10] B. Shan, C. Liu, Y. Guo, Y. Wang, W. Guo, Y. Zhang, and D. Wang, "A multi-layer stacked microfluidic tactile display with high spatial resolution," *IEEE Transactions on Haptics*, 2024.
- [11] Y. Wang, J. Liang, J. Yu, Y. Shan, X. Huang, W. Lin, Q. Pan, T. Zhang, Z. Zhang, Y. Gao *et al.*, "Multiscale haptic interfaces for metaverse," *Device*, 2024.
- [12] H. Inc., "HaptX Gloves G1," <https://haptx.com/gloves-g1/>, 2025, accessed: 2025-02-11.
- [13] D. P. Holland, E. J. Park, P. Polygerinos, G. J. Bennett, and C. J. Walsh, "The soft robotics toolkit: Shared resources for research and design," *Soft Robotics*, vol. 1, no. 3, pp. 224–230, 2014.
- [14] A. Shtarbanov, "Flowio development platform—the pneumatic "raspberry pi" for soft robotics," in *Extended abstracts of the 2021 CHI conference on human factors in computing systems*, 2021, pp. 1–6.
- [15] B. J. Caasenbrood, F. E. Van Beek, H. K. Chu, and I. A. Kuling, "A desktop-sized platform for real-time control applications of pneumatic soft robots," in *2022 IEEE 5th International Conference on Soft Robotics (RoboSoft)*. IEEE, 2022, pp. 217–223.
- [16] C. XR., "haptx-g1-mobile-single," <https://channelxr.com/products/haptx-gloves-g1?variant=48733998154044>, 2025, accessed: 2025-02-11.
- [17] C. Pacchierotti and D. Prattichizzo, "Cutaneous/tactile haptic feedback in robotic teleoperation: Motivation, survey, and perspectives," *IEEE Transactions on Robotics*, 2023.
- [18] A. Russomanno, S. O'Modhrain, R. B. Gillespie, and M. W. Rodger, "Refreshing refreshable braille displays," *IEEE transactions on haptics*, vol. 8, no. 3, pp. 287–297, 2015.
- [19] A. S. Walker and S. Sangelkar, "Design exploration of affordable refreshable braille display technology for low-income visually impaired users," in *International Design Engineering Technical Conferences and Computers and Information in Engineering Conference*, vol. 58134. American Society of Mechanical Engineers, 2017, p. V02BT03A012.
- [20] C. Travassos, A. Sayal, B. Direito, J. Pereira, T. Sousa, and M. Castelo-Branco, "Assessing mr-compatibility of somatosensory stimulation devices: A systematic review on testing methodologies," *Frontiers in Neuroscience*, vol. 17, p. 1071749, 2023.
- [21] L. A. Jones and N. B. Sarter, "Tactile displays: Guidance for their design and application," *Human factors*, vol. 50, no. 1, pp. 90–111, 2008.
- [22] P. Yu, L. C. Batteas, T. Ferris, M. C. Hipwell, F. Quek, and R. F. Friesen, "Investigating passive presentation paradigms to approximate active haptic palpation," *IEEE Transactions on Haptics*, 2024.
- [23] Programmable-air. Accessed: 2025-02-11. [Online]. Available: <https://www.programmableair.com/>
- [24] T. R. Young, M. S. Xavier, Y. K. Yong, and A. J. Fleming, "A control and drive system for pneumatic soft robots: Pneuord," in *2021 IEEE/RSJ International Conference on Intelligent Robots and Systems (IROS)*. IEEE, 2021, pp. 2822–2829.
- [25] Pneumatic controller. Accessed: 2025-02-11. [Online]. Available: <https://hdlc.mechanical.illinois.edu/open-source-materials/exo-test-bed/pneumatic-controller/>
- [26] Pneuduino. Accessed: 2025-02-11. [Online]. Available: <https://pneuduino.org/>
- [27] Q. Gao, J. Wang, Y. Zhu, J. Wang, and J. Wang, "Research status and prospects of control strategies for high speed on/off valves," *Processes*, vol. 11, no. 1, p. 160, 2023.
- [28] F. E. van Beek, Q. P. Bisschop, and I. A. Kuling, "Validation of a soft pneumatic unit cell (puc) in a vr experience: a comparison between vibrotactile and soft pneumatic haptic feedback," *IEEE Transactions on Haptics*, 2023.
- [29] L. C. L. van Laake, M. Alberts, F. E. van Beek, and I. A. Kuling, "A large area soft robotic haptic display," in *2024 IEEE 7th International Conference on Soft Robotics (RoboSoft)*. IEEE, 2024, pp. 728–733.
- [30] B. Stephens-Fripp, A. Israr, and C. Rognon, "A multichannel pneumatic analog control system for haptic displays: Multichannel pneumatic analog control system (mpacs)," in *Extended Abstracts of the 2021 CHI Conference on Human Factors in Computing Systems*, 2021, pp. 1–7.
- [31] R. Velázquez, E. Pissaloux, M. Hafez, and J. Szewczyk, "Toward low-cost highly portable tactile displays with shape memory alloys," *Applied Bionics and Biomechanics*, vol. 4, no. 2, pp. 57–70, 2007.
- [32] S. Hossain, A. A. Raied, A. Rahman, Z. R. Abdullah, D. Adhikary, A. R. Khan, A. Bhattacharjee, C. Shahnaz, and S. A. Fattah, "Text to braille scanner with ultra low cost refreshable braille display," in *2018 IEEE Global Humanitarian Technology Conference (GHTC)*. IEEE, 2018, pp. 1–6.
- [33] M. E. Vrablic, "Tactiontablet: affordable tactile graphics display," Ph.D. dissertation, Massachusetts Institute of Technology, 2020.
- [34] X. Wu, S.-H. Kim, H. Zhu, C.-H. Ji, and M. G. Allen, "A refreshable braille cell based on pneumatic microbubble actuators," *Journal of Microelectromechanical Systems*, vol. 21, no. 4, pp. 908–916, 2012.
- [35] J. Brown and F. Bello, "Design and characterisation of particle jamming-based variable stiffness displays using non-pneumatic actuators," in *2024 IEEE Haptics Symposium (HAPTICS)*. IEEE, 2024, pp. 379–384.
- [36] J. W. Booth, J. C. Case, E. L. White, D. S. Shah, and R. Kramer-Bottiglio, "An addressable pneumatic regulator for distributed control of soft robots," in *2018 IEEE International Conference on Soft Robotics (RoboSoft)*. IEEE, 2018, pp. 25–30.